Metallography, Microstructure, and Analysis (2019) 8:472–478
https://doi.org/10.1007/s13632-019-00555-y

TECHNICAL ARTICLE

Role of Heat Treatment on Grain Refinement and Microhardness of 9Cr–1Mo–V–Nb Steel

Chandan Pandey[1] · S. Sirohi[2] · M. M. Mahapatra[3] · Pradeep Kumar[4] · K. K. Bansal[2]

Received: 7 June 2018 / Revised: 27 February 2019 / Accepted: 17 May 2019 / Published online: 1 July 2019

Abstract

Effect of 'double austenitizing' (DN) on microstructure evolution and mechanical properties of martensitic 9Cr–1Mo–V–Nb (P91) steel were studied and compared with the 'conventional normalizing' (CN) process. In CN treatment, P91 steel is normalized at 1050 °C for 1 h, finally air cooled. In DN treatment, the first stage of normalizing was performed at 1050 °C/1 h/air cool. The second stage of normalizing was performed in the temperature range of 950–1150 °C for 1 h (950 °C-DN1, 1050 °C-DN2, 1150 °C-DN3), followed by water quenching. The grain size was measured 42 and 35 µm for CN and DN1 treatment, respectively. The double normalizing (DN) produced complete martensitic microstructure as a result of complete dissolution of precipitates. In DN-based heat treatment, optimized microstructure and mechanical properties were obtained for the sample that normalized at 950 °C, followed by water quenching.

Keywords Grain refinement · P91 steel · Heat treatment · Microstructure · Hardness

Introduction

9Cr–1Mo–V–Nb steel known as P91 steel is the most commonly used material for the power plant components operating in high temperature and pressure range about 550–620 °C and 250–300 bar [1–3]. 9Cr–1Mo–V–Nb steels offer excellent creep rupture strength as compared to plain 9Cr–1Mo steels and austenitic steels. It also offers better irradiation embrittlement, void swelling resistance, and superior yield strength at high temperature [4, 5]. 9Cr–1Mo–V–Nb steels were developed by altering the composition of plain 9Cr–1Mo steel [6]. Before put in the service, P91 steels are subjected to normalizing and tempering treatment to produce the optimum combination of the microstructure and mechanical properties, which further governs the creep rupture life and microstructure evolution during the prolonged creep exposure. The normalizing of the steel leads to the formation of the untempered lath martensite with high dislocation density, while tempering reaction results in the formation of tempered martensite with lath blocks, packets, grain boundaries, and carbide and carbonitrides precipitates [7, 8]. Pandey et al. [9] reported the size of coarse $M_{23}C_6$ precipitates in the range of 100–250 nm, while the size of intra-lath MX precipitates was in range of 10–40 nm [10]. An optimum selection of microstructure and heat treatment for P91 steel is an important step for stringent nuclear applications [11, 12]. The mechanical behavior and microstructural characteristic of the P91 steel are strongly governed by the heat treatment and their duration [5, 11, 13–17]. For P91 steel, austenitizing temperature was reported above A_{c3} (finish temperature of ferrite to austenite phase transformation) and in the temperature range of 1000–1050 °C while tempering in the range of 730–780 °C. Austenitizing at temperatures above A_{c3} results in the dissolution of $M_{23}C_6$ precipitates and lead to the formation of coarse grains [18]. To overcome the substantial grain growth of austenite, double austenitization heat treatment has been utilized by many of researchers for improving the Charpy toughness of P91 steel [4, 19]. The initial austenitizing deals with heating of steel

✉ Chandan Pandey
jscpandey@iitj.ac.in; chandanpy.1989@gmail.com

1 Department of Mechanical Engineering, IIT Jodhpur, NH 65 Nagaur Road, Karwar, Rajasthan 342037, India

2 Department of Mechanical Engineering, SRM IST Delhi NCR Campus Modinagar, Ghaziabad, Uttarpradesh 201204, India

3 School of Mechanical Sciences, Indian Institute of Technology, Bhubaneswar, Odisha 751013, India

4 Department of Mechanical and Industrial Engineering, Indian Institute of Technology Roorkee, Roorkee, Uttrakhand 247667, India

above the A_{c3} temperature as similar to the conventional normalizing treatment [4, 20–22]. This results in the formation of untempered lath martensite devoid of carbide precipitates [23, 24]. After the first stage of austenitizing, the second stage of austenitizing was performed to obtain homogeneous fine grains of austenite. Karthikeyan et al. [19] studied the effect of double normalizing effect on microstructure evolution of 9Cr–1Mo steel. Fine prior austenite grains (PAGs) with uniform tempered martensitic microstructure and better Charpy toughness were reported for the 'Double austenitization-based Normalizing and Tempering' (DNT) as compared to 'Conventional Normalizing and Tempering' (CNT) treatment. Grain refinement of material enhances the impact toughness and strength of material, while grain refinement might be the cause of poor creep strength, especially if it is driven by Coble creep mechanism. For dislocation climb creep mechanism (low temperature and high stress), it might be useful [25].

Microstructure and high-temperature mechanical properties of P91 steel are mainly governed by the processing history [26]. Thermal aging of P91 steel in the temperature range of 520–650 °C for long time causes a significant reduction in temperature strength properties [8, 27]. For long-term aging, microstructure faces the following changes such as martensite recovery, precipitation of intermetallic phase (Laves, Z-phase), coarsening of $M_{23}C_6$ precipitates, and impurity segregation along the boundaries. These result in the detonation of creep and impact toughness of material [28–31]. In P91 steel, long-term aging has resulted in the reduction in upper shelf energy (USE), and increase in ductile brittle transaction temperature (DBTT). Reduction in fracture toughness and impurity such as P- and S-based embrittlement was also observed [32, 33]. The objective of the current study is to study the effect of conventional normalizing (CN) and double normalizing (DN) treatment on the microstructure evolution and hardness of P91 steel.

Experiments and Methods

Heat Treatment

A 20-mm-thick steel P91 steel plate (chemical composition, wt.%: 0.10 C, 8.16 Cr, 0.71 Mo, 0.18 V, 0.30 Ni, 0.67 Mn, 0.19 Si, 0.02 P, 0.05 Nb, 0.02 N, balance Fe) was supplied in cast and forged conditions. The typical optical micrograph of the P91 steel confirms the partially tempered martensite with lath block structure and precipitates (Fig. 1). The precipitates are shown in Fig. 1b and are found to be decorated along the lath boundaries.

The plate was subjected to conventional normalizing and double-austenitizing treatment as per Fig. 2.

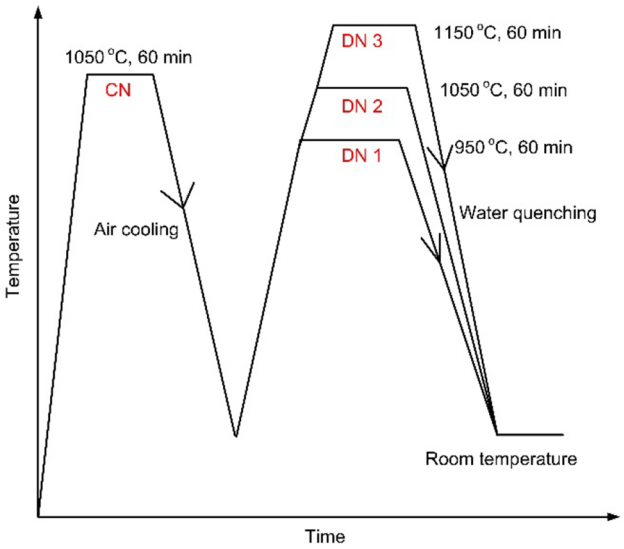

Fig. 2 Schematic diagram showing the heat treatment of P91 steel

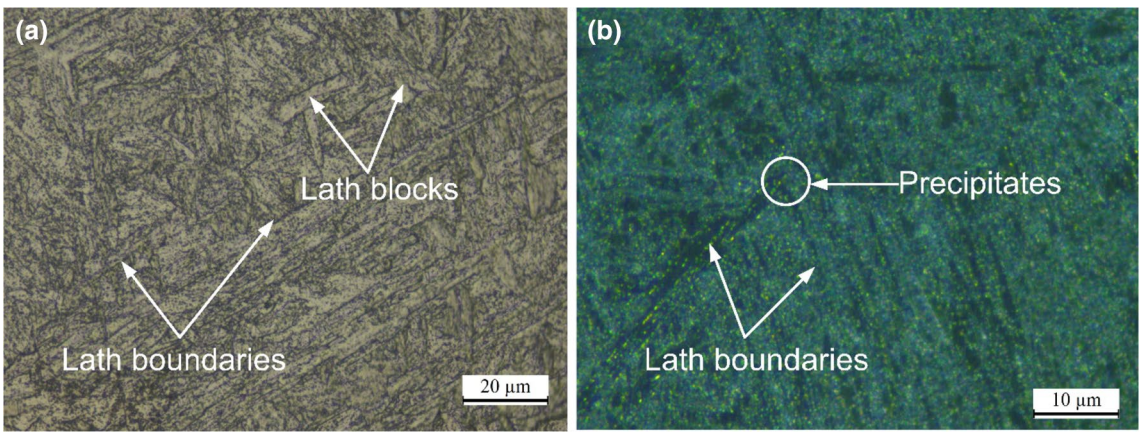

Fig. 1 Optical micrograph of P91 steel (**a**) blocks and boundaries; (**b**) precipitates

- CN—'1050 °C/1 h/air cool'
- DN1—'1050 °C/1 h/air cool, 950 °C/1 h/water quench'
- DN2—'1050 °C/1 h/air cool, 1050 °C/1 h/water quench'
- DN3—'1050 °C/1 h/air cool, 1150 °C/1 h/water quench.'

Microstructure Characterization and Hardness Tests

From the heat-treated plate, specimens are sectioned for the metallographic study. The sectioned samples were polished and etched in Vilella's reagent (100 ml of ethanol + 1 g of picric acid + 5 ml of hydrochloric acid) for optical microscope and scanning electron micrograph (SEM). The microhardness test was performed on the etched sample using OmniTech S. Auto microhardness tester with a load of 500 g and dwell time of 10 s.

Results and Discussion

As-Received Material

Steel in the cast and forged conditions is discussed in the previous works [13, 34, 35]. As-received material microstructure shows the presence of columnar lath, martensitic blocks and packets. The Cr-, Fe- and Mo-rich carbide precipitates are clearly observed along the packet and lath boundaries, while fine MX precipitates are observed inside the intra-lath region. A typical SEM micrograph of P91 steel (Fig. 3) shows the distribution and morphology of precipitates. Figure 3a shows the decoration of the precipitates along the lath blocks. Figure 3b indicates the presence of coarse precipitates along block boundaries of spherical, rectangular, and needle shapes. The size varies from 100 to 300 nm. The fine precipitates of spherical shape are measured in the range of 25–50 nm. The coarse precipitates are $M_{23}C_6$ carbides, where M is Mo, Cr, and W, and fine precipitates are M(C,N), where M can Nb and/or V [36].

Grain Refinement Analysis

Optical Microscopy

The optical micrograph corresponding to the different heat treatments is depicted in Fig. 4. The microstructure exhibited the untempered martensite with typical martensitic lath blocks and packets. Three distinct morphologies (lath blocks, lath packets, and PAGs) of the microstructure were observed. The prior austenite grains (PAGs) consisted of a number of lath packets having a number of lath blocks. Lath blocks inside the packets show a similar orientation. In CN condition, the lath blocks are clearly observed. The strength of the P91 steel depends on the solid solution hardening and precipitation hardening. The normalizing of the steel results in the dissolution of the precipitates in matrix that leads to the increase in solid solution strengthening. The dissolution of precipitates makes the PAGBs free and allows the grain to be coarse. In DN1 treatment, the micrograph looks similar as obtained in CN condition. For DN2 treatment, the lath blocks show different morphologies. The coarsening of the grains is also observed as compared to the DN1 treatment. The increase in the normalizing temperature leads to the dissolution of the precipitates and formation of the coarse grains. At high normalizing temperature (about 1050 °C), the Cr-rich $M_{23}C_6$ precipitates get dissolved completely. However, some fine Nb-rich precipitates remain in the microstructure that shows the higher thermal stability of these particles (up to 1250 °C). The coarsening of grains is clearly observed with the change in the heat treatment condition from DN1 to DN3. The grain size was measured 42 µm for the CN treatment. The grain sizes for the DN1, DN2, and DN3 treatments were 35, 50, and 62 µm, respectively.

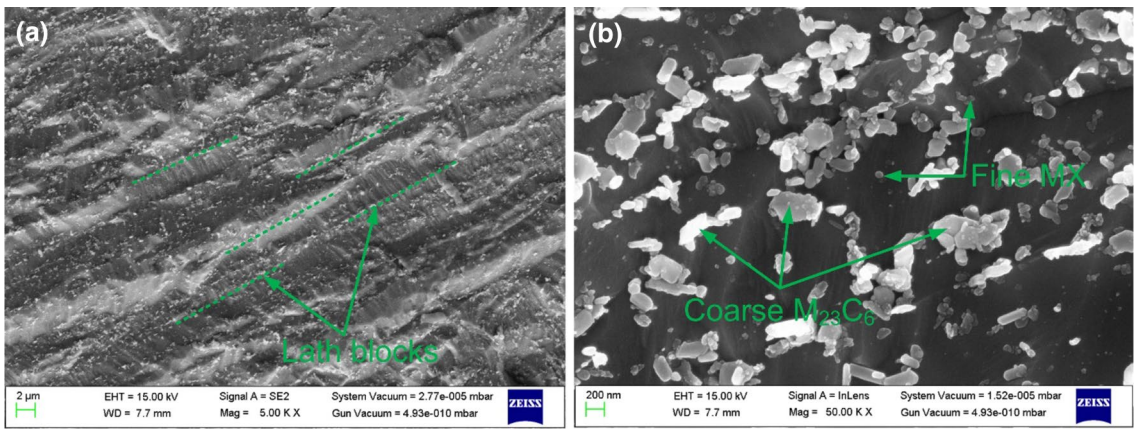

Fig. 3 SEM micrograph of C&F P91 steel (**a**) lath blocks and decoration of precipitates along block boundaries; (**b**) morphology of precipitates

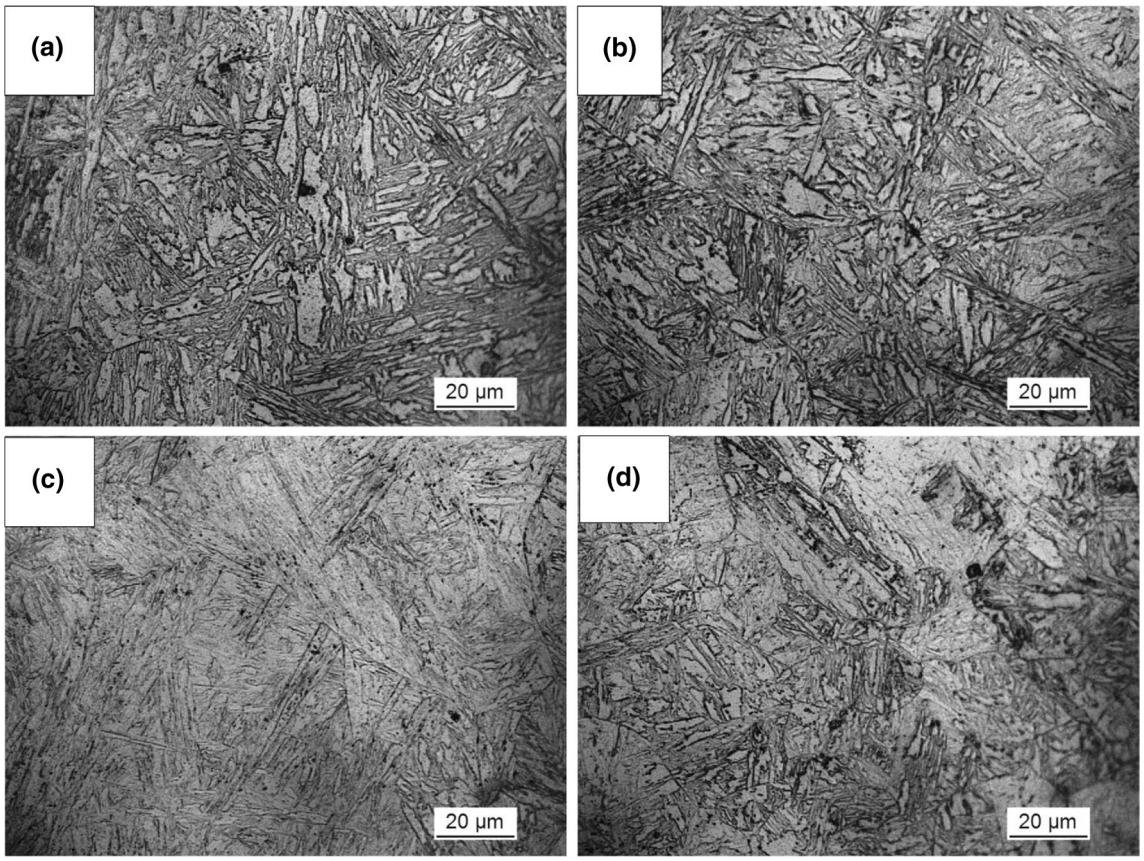

Fig. 4 Optical micrograph for different operating states (**a**) CN, (**b**) DN1, (**c**) DN2, (**d**) DN3

Figure 4a, b indicates the PAGs for CN and DN1 treatments, respectively. In DN 2 and DN 3 treatments, it becomes difficult to trace the PAGs as a result of the coarsening of grains.

Scanning Electron Microscopy

Figure 5 indicates the SEM micrograph of P91 steel in different heat treatment conditions. In the CN condition, the coarse undissolved precipitates, PAGs and lath blocks are observed. The higher precipitate density along the lath blocks is clearly observed. In the DN1 treatment, the distinct PAGBs and lath blocks with precipitates are observed. The coarsening behavior of the steel is clearly observed with change in heat treatment from DN1 to DN2. In the DN 2 treatment, the micrograph looks similar to DN1. Figure 5d shows the lath blocks for the DN3 treatment. The PAGs are not observed due to coarse grain size.

Microhardness

Figure 6 shows the variation in hardness for varying heat treatments. Solid solution hardening and precipitation hardening are the possible mechanisms that govern the mechanical behavior of the P91 steel. For CN, hardness was measured as 335 HV. The heat treatment has had a strong influence on the hardness of the P91 steel [37]. The normalizing of steel leads to the solid solution hardening due to precipitates dissolution. The hardness also depends on the grain size of the steel [14]. The higher density of the precipitates and nucleation of the precipitates mainly occurred along the PAGBs and lath boundaries. The coarsening behavior of the steel leads to the reduction in grain boundaries per unit area. That also affects the fraction area of precipitates directly. The reduction in availability of the grain boundaries leads to the lower availability of the precipitates nucleation sites and also to the reduction in the fraction area of the precipitates. The reduction in the fraction area of precipitates results in higher solid solution hardening. As compared to the CN treatment, a negligible change in microhardness was observed for the DN1 treatment due to almost similar grain size. For DN1 treatment. For DN2 and DN3 treatments, a noticeable change in hardness was observed as compared to CN and DN1 treatments. In DN2 and DN3 treatments, a higher portion of martensite in the microstructure, due to

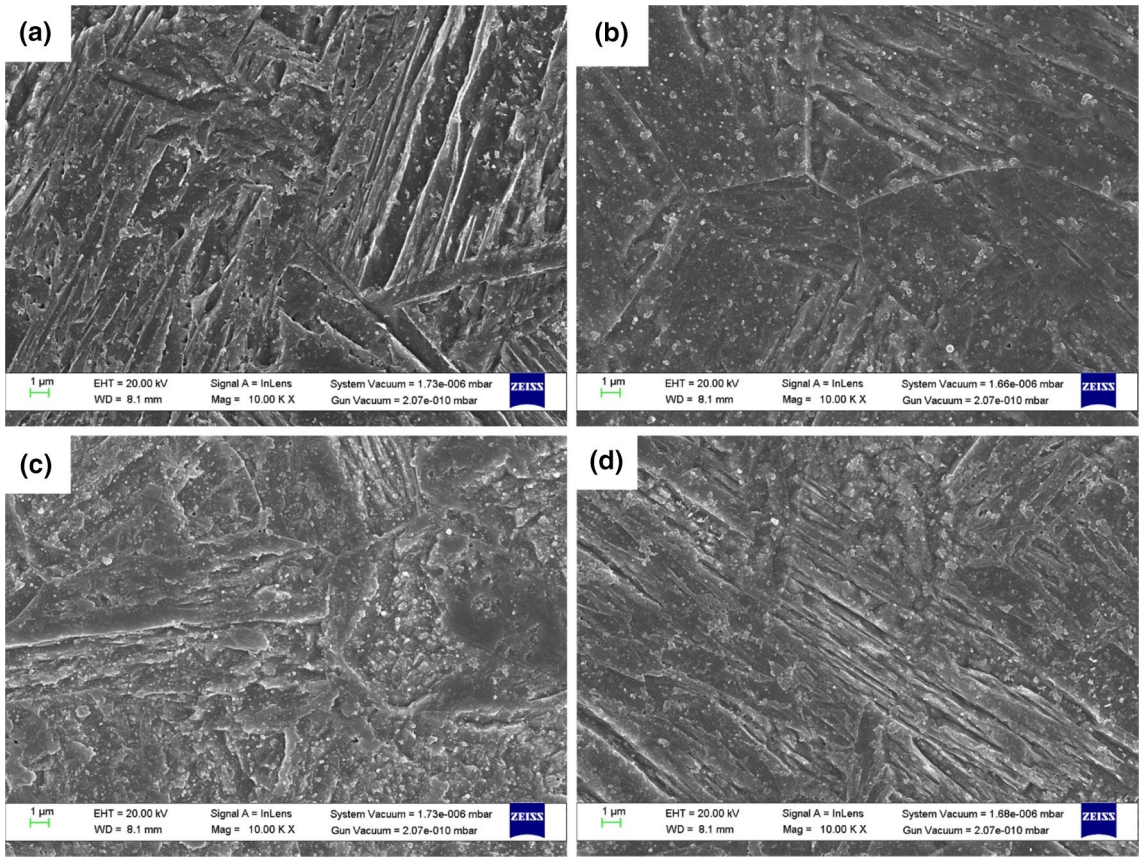

Fig. 5 Secondary electron micrograph for different operating states (**a**) CN, (**b**) DN1, (**c**) DN2, (**d**) DN3

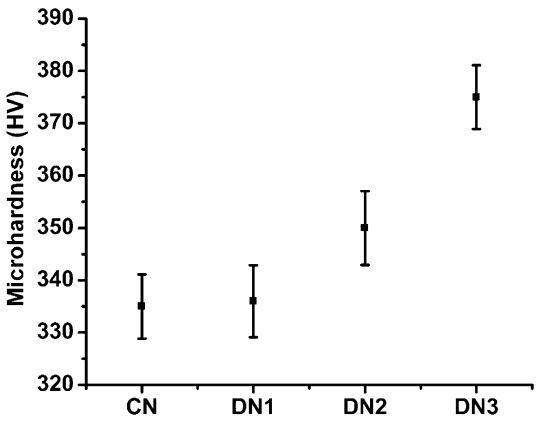

Fig. 6 Hardness variation for different operating states

the water quenching, leads to drastic increase in hardness. The increase in hardness from DN2 to DN3 may be due to the higher dissolution of carbides, which enhances the solid solution strengthening in the martensite. On the other hand, DN1 has a lower hardness because the quenching temperature (950 °C) was too low.

Conclusions

From the present work, the following conclusion can be drawn:

- The as-received cast and forged P91 steel showed the tempered martensitic microstructure with typical columnar lath blocks and precipitates along with it.
- The grain refinement is observed for the DN1 treatment, and grain size was reduced from 42 to 35 µm; hence, optimum grain refinement was considered for the DN1 treatment.
- The 'double austenitizing' resulted in the formation of untempered martensitic lath microstructure. The precipitate gets dissolved as a result of increase in the normalizing temperature from 950 to 1150 °C. The coarse $M_{23}C_6$ precipitates were also dissolved at higher normalizing temperature of 1150 °C.
- The hardness measured for the DN1 treatment was 339 HV. The hardness increased with the change in the operating condition from the DN1 to DN3 treatments. The maximum hardness of 375 HV was measured for the DN3 treatment. In DN3, maximum hardness was attrib-

uted to a higher portion of martensite in the microstructure, due to the water quenching and higher dissolution of carbides, which enhances the solid solution strengthening in the martensite.

References

1. C. Pandey, M.M. Mahapatra, P. Kumar, N. Saini, Effect of strain rate and notch geometry on tensile properties and fracture mechanism of creep strength enhanced ferritic P91 steel. J. Nucl. Mater. **498**, 176–186 (2018). https://doi.org/10.1016/j.jnucmat.2017.10.037
2. R.L. Klueh, B. Van Der Schaaf, M. Victoria, Ferritic/martensitic steels: overview of recent results. J. Nucl. Mater. **311**, 455–465 (2008)
3. R.L. Klueh, A.T. Nelson, Ferritic/martensitic steels for next-generation reactors. J. Nucl. Mater. **371**, 37–52 (2008). https://doi.org/10.1016/j.jnucmat.2007.05.005
4. T. Karthikeyan, M. Kumar, R. Mythili, S.P. Selvi, A. Moitra, S. Saroja, Effect of prior-austenite grain refinement on microstructure, mechanical properties and thermal embrittlement of 9Cr–1Mo–0.1C steel. J. Nucl. Mater. **494**, 260–277 (2017). https://doi.org/10.1016/j.jnucmat.2017.07.019
5. C. Pandey, M.M. Mahapatra, P. Kumar, N. Saini, A. Srivastava, Microstructure and mechanical property relationship for different heat treatment and hydrogen level in multi-pass welded P91 steel joint. J. Manuf. Process. **28**, 220–234 (2017). https://doi.org/10.1016/j.jmapro.2017.06.009
6. C. Pandey, M.M. Mahapatra, Effect of Heat Treatment on Microstructure and Hot Impact Toughness of Various Zones of P91 Welded Pipes. J. Mater. Eng. Perform. **25**, 2195–2210 (2016). https://doi.org/10.1007/s11665-016-2064-x
7. C. Pandey, A. Giri, M.M. Mahapatra, Effect of normalizing temperature on microstructural stability and mechanical properties of creep strength enhanced ferritic P91 steel. Mater. Sci. Eng., A **657**, 173–184 (2016). https://doi.org/10.1016/j.msea.2016.01.066
8. C. Pandey, M.M. Mahapatra, Effect of long-term ageing on the microstructure and mechanical properties of creep strength enhanced ferritic P91 steel. Trans. Indian Inst. Met. **69**, 1657–1673 (2016). https://doi.org/10.1007/s12666-015-0826-z
9. C. Pandey, M.M. Mahapatra, P. Kumar, N. Saini, Comparative study of autogenous tungsten inert gas welding and tungsten arc welding with filler wire for dissimilar P91 and P92 steel weld joint. Mater. Sci. Eng., A **712**, 720–737 (2018). https://doi.org/10.1016/j.msea.2017.12.039
10. C.G. Panait, A. Zielinska-Lipiec, T. Koziel, A. Czyrska-filemonowicz, A.F. Gourgues-Lorenzon, W. Bendick, Evolution of dislocation density, size of subgrains and MX-type precipitates in a P91 steel during creep and during thermal ageing at 600 °C for more than 100,000h. Mater. Sci. Eng., A **527**, 4062–4069 (2010). https://doi.org/10.1016/j.msea.2010.03.010
11. C. Pandey, A. Giri, M.M. Mahapatra, Evolution of phases in P91 steel in various heat treatment conditions and their effect on microstructure stability and mechanical properties. Mater. Sci. Eng., A **664**, 58–74 (2016). https://doi.org/10.1016/j.msea.2016.03.132
12. C. Pandey, M. Mahapatra, Evolution of phases during tempering of P91 steel at 760 for varying tempering time and their effect on microstructure and mechanical properties. Proc. Inst. Mech. Eng. Part E J. Process Mech. Eng. **664**, 58–74 (2016). https://doi.org/10.1177/0954408916656678
13. C. Pandey, M.M. Mahapatra, P. Kumar, N. Saini, Characterization of Cast and Forged (C&F) Gr. 91 steel in different heat treatment condition. Trans. Indian Inst. Met. (2017). https://doi.org/10.1007/s12666-017-1144-4
14. C. Pandey, M.M. Mahapatra, P. Kumar, N. Saini, J.G. Thakre, Nano-size particle evolution during heat treatment of P91 steel and their effect on micro hardness. Trans. Indian Inst. Met. (2017). https://doi.org/10.1007/s12666-017-1215-6
15. R.L. Klueh, D.J. Alexander, Heat treatment effects on toughness of 9Cr–1MoVNb and 12Cr–1MoVW steels irradiated at 365 °C. J. Nucl. Mater. **191–194**, 896–900 (1992). https://doi.org/10.1016/0022-3115(92)90602-H
16. N. Zavaleta Gutiérrez, H. De Cicco, J. Marrero, C.A. Danón, M.I. Luppo, Evolution of precipitated phases during prolonged tempering in a 9%Cr1%MoVNb ferritic-martensitic steel: Influence on creep performance. Mater. Sci. Eng. A. **528**, 4019–4029 (2011). https://doi.org/10.1016/j.msea.2011.01.116
17. C. Hurtado Noreña, P. Bruzzoni, Effect of microstructure on hydrogen diffusion and trapping in a modified 9% Cr–1% Mo steel. Mater. Sci. Eng. A. **527**, 410–416 (2010). https://doi.org/10.1016/j.msea.2009.08.025
18. N. Saini, C. Pandey, M. Mohan, R.S. Mulik, Evolution of nano-size precipitates during tempering of 9Cr–1Mo–1W–V–Nb steel and their influence on mechanical properties. Mater. Sci. Eng., A **711**, 37–43 (2018). https://doi.org/10.1016/j.msea.2017.11.011
19. T. Karthikeyan, V. Thomas Paul, S. Saroja, A. Moitra, G. Sasikala, M. Vijayalakshmi, Grain refinement to improve impact toughness in 9Cr–1Mo steel through a double austenitization treatment. J. Nucl. Mater. **419**, 256–262 (2011). https://doi.org/10.1016/j.jnucmat.2011.08.010
20. C. Wang, M. Wang, J. Shi, W. Hui, H. Dong, Effect of microstructural refinement on the toughness of low carbon martensitic steel. Scr. Mater. **58**, 492–495 (2008). https://doi.org/10.1016/j.scriptamat.2007.10.053
21. B.V. Narasimha Rao, G. Thomas, Design of Fe/4Cr/0.4C martensitic steels eliminating quench cracking. Mater. Sci. Eng. **20**, 195–202 (1975). https://doi.org/10.1016/0025-5416(75)90149-4
22. J. Liu, H. Yu, T. Zhou, C. Song, K. Zhang, Effect of double quenching and tempering heat treatment on the microstructure and mechanical properties of a novel 5Cr steel processed by electroslag casting. Mater. Sci. Eng., A **619**, 212–220 (2014). https://doi.org/10.1016/j.msea.2014.09.063
23. T. Hirose, K. Shiba, T. Sawai, S. Jitsukawa, M. Akiba, Effects of heat treatment process for blanket fabrication on mechanical properties of F82H. J. Nucl. Mater. **329–333**, 324–327 (2004). https://doi.org/10.1016/j.jnucmat.2004.04.047
24. X. Xiong, F. Yang, X. Zou, J. Suo, Effect of twice quenching and tempering on the mechanical properties and microstructures of SCRAM steel for fusion application. J. Nucl. Mater. **430**, 114–118 (2012). https://doi.org/10.1016/j.jnucmat.2012.06.047
25. R.L. Klueh, Elevated temperature ferritic and martensitic steels and their application to future nuclear reactors. Int. Mater. Rev. **50**, 287–310 (2005). https://doi.org/10.1179/174328005X41140
26. B.K. Choudhary, Influence of processing route and section size on elevated temperature tensile properties of 9Cr–1Mo ferritic steel. High Temp. Mater. Process. **31**, 27–35 (2012)
27. B.K. Choudhary, K.B. Sankara, S.L. Mannan, B.P. Kashyap, Influence of prior thermal ageing on tensile deformation and fracture behaviour of forged thick section 9Cr ± 1Mo ferritic steel. J. Nucl. Mater. **273**, 315–325 (1999)
28. C. Pandey, M.M. Mahapatra, P. Kumar, R.S. Vidyrathy, A. Srivastava, Microstructure-based assessment of creep rupture behaviour of cast-forged. Mater. Sci. Eng., A **695**, 291–301 (2017). https://doi.org/10.1016/j.msea.2017.04.037
29. C. Pandey, M.M. Mahapatra, P. Kumar, N. Saini, Effect of creep phenomena on room-temperature tensile properties of cast and

forged P91 steel. Eng. Fail. Anal. **79**, 385–396 (2017). https://doi.org/10.1016/j.engfailanal.2017.05.025
30. V.T. Paul, S. Saroja, M. Vijayalakshmi, Microstructural stability of modified 9Cr–1Mo steel during long term exposures at elevated temperatures. J. Nucl. Mater. **378**, 273–281 (2008). https://doi.org/10.1016/j.jnucmat.2008.06.033
31. K.J. Harrelson, S.H. Rou, R.C. Wilcox, Impurity element effects on the toughness of 9Cr–1Mo steel. J. Nucl. Mater. **141–143**, 508–512 (1986). https://doi.org/10.1016/S0022-3115(86)80091-5
32. F.W. Noble, B.A. Seniort, B.L. Eyre, The effect of Phosphorus on 9 Cr–Mo Steels. Acta Mater. Mater. **38**, 709–717 (1990)
33. S. Sathyanarayanan, J. Basu, A. Moitra, G. Sasikala, Effect of thermal aging on ductile-brittle transition temperature of modified 9Cr–1Mo steel evaluated with reference temperature approach under dynamic loading condition. Metall. Mater. Trans. A **44**, 2141–2155 (2013). https://doi.org/10.1007/s11661-012-1510-0
34. C. Pandey, N. Saini, M.M. Mahapatra, P. Kumar, Study of the fracture surface morphology of impact and tensile tested cast and forged (C&F) Grade 91 steel at room temperature for different heat treatment regimes. Eng. Fail. Anal. **71**, 131–147 (2016). https://doi.org/10.1016/j.engfailanal.2016.06.012
35. C. Pandey, M.M. Mahapatra, P. Kumar, N. Saini, Diffusible Hydrogen Level in deposited metal and their effect on tensile properties and flexural strength of P91 steel. J. Eng. Mater. Technol. **139**, 1–11 (2017). https://doi.org/10.1115/1.4035764
36. C.G. Panait, W. Bendick, A. Fuchsmann, A.F. Gourgues-Lorenzon, J. Besson, Study of the microstructure of the Grade 91 steel after more than 100,000 h of creep exposure at 600 °C. Int. J. Press. Vessel. Pip. **87**, 326–335 (2010). https://doi.org/10.1016/j.ijpvp.2010.03.017
37. C. Pandey, M.M. Mahapatra, P. Kumar, N. Saini, Homogenization of P91 weldments using varying normalizing and tempering treatment. Mater. Sci. Eng., A **710**, 86–101 (2018). https://doi.org/10.1016/j.msea.2017.10.086